PERGAMON

Journal of Structural Geology 22 (2000) 1559–1564

JOURNAL OF STRUCTURAL GEOLOGY

www.elsevier.nl/locate/jstrugeo

The Jülich neutron diffractometer and data processing in rock texture investigations

E. Jansen*, W. Schäfer, A. Kirfel

Mineralogisch-Petrologisches Institut, Universität Bonn, 53115 Bonn, Germany

Received 29 November 1999; accepted 3 May 2000

Abstract

The texture diffractometer SV7-b which is operated at the Forschungszentrum Jülich as a user and service instrument has been improved with respect to the efficiency of the position-sensitive detector system and to the variety of wavelengths available. Instrumental aspects of data collection and different methods of data processing for pole figure evaluation are discussed. Recent examples of texture investigations on geological materials are presented for quartz, hematite, hematite-quartz, orthopyroxen-quartz and anorthosite rocks. © 2000 Elsevier Science Ltd. All rights reserved.

1. Introduction

During the last two decades neutron diffraction has been developed to a well-established technique in geological texture analysis. Owing to the high penetration capability of neutrons large specimens of several cm^3 volume can be used for pole figure studies with high grain statistics, even for coarse-grained material (Wenk et al., 1984). Linear detectors are used to meet the special requirements for investigations of geological samples which often show reflection-rich diffraction patterns due to both the low crystal symmetries of many minerals (Wenk et al., 1986) and the multiphase compositions of most rocks (Schäfer et al., 1991). Using these detectors, one can recognize superpositions of reflections which may then be deconvoluted into individual pole figures by means of appropriate data analysis (see for example Will et al., 1989). Furthermore, one can simultaneously collect the data for a manifold of different pole figures being required for reliable calculations of three-dimensional orientation distribution functions. This paper aims (1) to inform on the recently modified instrumental setup of the texture facility of the twin diffractometer SV7 which is operated by the University of Bonn as a service instrument at the Forschungszentrum Jülich (Schäfer et al., 1997), (2) to briefly discuss specific procedures of data handling and pole figure preparation, and (3) to illustrate the performance of the method by some recent results of texture investigations.

2. Instrumental aspects

The texture diffractometer SV7-b (Fig. 1) is installed at a thermal neutron beam inside the experimental hall of the FRJ-2 research reactor. The instrument can be operated with different monochromator crystals covering a wavelength range from 0.9 to 2.3 Å (see Table 1). The recent extension to the regime of longer wavelengths, from 1.5 to 2.3 Å, which is achieved by PG-002 combined with an appropriate ($\lambda/2$)-filter suppressing higher order contaminations, was performed particularly in view of improved experimental pole figure separations for investigations of geological material. Longer wavelengths result in a shift of the highest instrumental resolution ($\Delta d/d = 1.3\%$ at $2\Theta = 40°$) from d-spacings of about 1.5 Å ($\lambda = 1.0$ Å) to d-spacings of about 4 Å (with $\lambda = 2.3$ Å). The latter regime is better matching d-spacings of the principal lattice planes of minerals and multiphase rocks that are privileged for pole figure representations and texture interpretations.

The texture diffractometer is now being equipped with the largest version of the position-sensitive scintillation detector of the JULIOS-type (Müller et al., 1996). The sensitive detector window provides an area of 940×75 mm^2, being about four times larger than that of the previously installed standard version of JULIOS. In particular, the increase in the vertical aperture of the detector, from 25 to 75 mm, results in a substantial increase of recorded neutrons which allows a reduction of the measuring time for a pole figure scanning by a factor of 2 on average, maintaining experimental counting statistics. The detector is installed on a free rotating base plate at a distance of about 100 cm

* Corresponding author.

0191-8141/00/$ - see front matter
PII: S0191-8141(00)00057-2

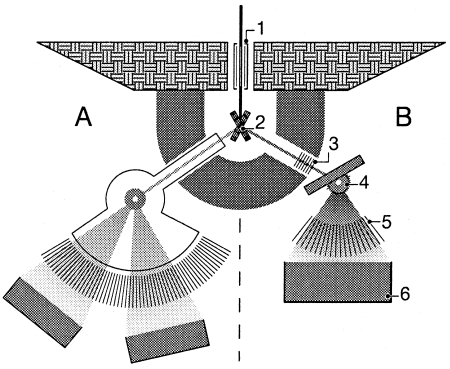

Fig. 1. The twin instrument SV7 with powder diffractometer (A) and texture diffractometer (B). The main components of (B): primary collimator (1), monochromator crystal (2), λ/2-filter (3), sample on Eulerian cradle (4), radial collimator (5), and linear position-sensitive detector (6).

from the sample which itself is mounted in a full-circle Eulerian cradle. In fixed position, the linear detector covers a section of $\Delta 2\Theta = 50°$. Under normal conditions this detector extension permits the collection of data sufficient for all necessary pole figures in only one sample scan.

Background scattering into the relatively large detector has been effectively reduced by installing (1) a funnel-shaped outer shielding around the free neutron flight path between sample and detector, and (2) an efficient beam absorber which prevents any scattering of primary transmitted neutrons into the detector. These measures resulted in an improvement of the mean peak to background ratio by a factor of about 2. Optionally, the secondary shielding can be substituted by an oscillating radial collimator device consisting of thin neutron-absorbing sheets with about 11.5 mm spacings at the sample side. Besides background reduction, this radial collimator reduces the dependence of the instrumental resolution (i.e. width of Bragg peaks) from the sample size for specimen dimensions >10 mm. A further benefit of the radial collimator is the elimination of contamination in the diffraction patterns caused by additional sample environments, e.g. furnaces, cryostats or pressure cells.

Table 1
Instrumental details

Primary collimator	Soller 0.2°
Take-off angle	40°
Monochromators	Cu-220, Ge-311, Ni-200, Cu-111 or PG-002 (pyrolythic graphite)
Wavelengths	0.9 Å to 2.3 Å
Filter	Pyrolythic graphite
2θ-range	2° to 90°
Range of d-spacings	0.7 Å to 25 Å
Radial collimator	Oscillating; $r_{min} = 440$ mm, $r_{max} = 920$ mm, spacing between laminae = 1.5°
Mean flux at sample position	1×10^6 n/cm^2 s
Max. beam size	25×40 mm^2
Detector	^{6}Li-scintillation glass; linear position sensitive; sensitive area: 940×75 mm^2
Δd/d-resolution	1.3% at 1000 mm detector distance

In principle, the pole figure scanning grids, characterized by stepwidths $\Delta\varphi$ and $\Delta\chi$ on the Eulerian cradle, can be chosen according to individual requirements of crystallinity and microstructure. For most geological specimens, however, a model pattern approximating an equal area scan is provided as standard. It consists of about 500 individual sample orientations (φ, χ) which under consideration of the Eulerian cradle and peak positions ω and 2Θ, respectively, have to be converted into pole figure coordinates (α, β), because, owing to the use of a linear detector, the reflections are not generally measured in bisecting geometry (Bunge et al., 1984; Wenk et al., 1986). In most cases, the pole figures are constructed by interpolation for points of an equispaced $5° \times 5°$ (α, β)-grid.

Usual measuring times are between 1 and 3 min per sample position depending on sample size, symmetry and chemical compositions. The samples are generally prisms, cylinders or cubes with volumes between about 1 and 10 cm^3. The total measuring time for a complete set of about 20 pole figures per rock sample amounts to between 8 and 24 h.

3. Pole figure data processing

The Jülich pole figure data processing is adapted to the special potential of the position-sensitive detector. The fact that complete diffraction patterns are automatically recorded for each orientation during sample scanning allows several alternatives in data handling for pole figure synthesis: (1) the conventional method using only the intensities of the peak maxima similar to the procedure applied at single counter diffractometers; (2) the integration method working with integrated intensities of single peaks or of arrays of peaks which can be unambiguously assigned to individual Bragg reflections; and (3) the profile fitting method which provides a deconvolution of overlapping reflections by peak profile analysis and subsequent integration of each separated peak profile. The choice of any of these methods depends on the specimen, i.e. on the quality and appearance of the diffraction patterns and on the complexity of the texture analysis.

The conventional method (1) is confined to specimens of high crystal symmetry showing well-separated diffraction peaks that provide sufficient counting statistics. Principally, method (1) means a waste of data which, however, are exploited by methods (2) and (3).

The integration method (2) provides a gain in pole figure statistics since integrated rather than peak maxima intensities are used. Furthermore, this method is more reliable with respect to possible peak shifts which occasionally occur during scannings of large and inhomogeneous specimens, e.g. multiphase rocks. Frequently, those shifts remain unconsidered in the conventional method (1) or remain even unnoticed when a single counter detector is used.

The profile fitting method (3) is especially suited to the needs of texture analyses of specimens showing

reflection-rich diffraction patterns with usually severe peak overlapping. This applies, in particular, to geological material that often contains several mineral phases and/or is composed of mineral components with low crystal symmetry. Mathematical peak profile analysis is then required in order to obtain a sufficient number of individual (separated) pole figures for the calculation of a reliable orientation distribution function. With respect to this kind of pole figure data analysis, a special procedure of pattern decomposition has been developed in our institute taking care of an efficient handling of the huge amounts of data collected in the position-sensitive detector (see for example Wenk et al., 1986; Will et al., 1992).

The experimental pole figures are finally used to calculate a three-dimensional orientation distribution function (ODF) which in turn allows the recalculation of pole figures, even of those lattice planes which cannot be directly measured either due to too strong peak overlap in the diffraction pattern, or for space group extinction or intensity reasons. (A notorious example is the (000l) of the trigonal quartz structure.) These ODF calculations are performed by using the program MENTEX by Schäben (1994) or, alternatively, the program MULTEX by Helming (1996).

4. Examples and results

SV7-b is a dedicated national texture diffractometer funded by the Federal Minister for Education and Research (BMBF). It is operated as a service instrument that is open to external users and university institutes. In the following sections we present results of recent texture investigations carried out on SV7-b in co-operation with external groups working on geological projects.

5. Naturally deformed quartzite

The volume texture of a naturally deformed quartzite collected from the (Pan-African) Nosib quartzite of the Tomakas area in the Kaoko belt, North-West Namibia, has been analysed by neutron diffraction for a more complete description of the texture than could be obtained by universal stage microscopy (Ghildiyal et al., 1999). The microstructure indicates a spectrum of grain size from 0.03 to 0.83 mm and shows a sharp preferred orientation in the lineation direction.

A total of 14 pole figures covering d-spacings between 1.2 and 5.8 Å has been measured on an almost cubic sample of dimensions $2 \times 2 \times 2$ cm^3. The experimental pole figures {10-10} and {11-20} describe the preferred orientations of the first order prism {m} and second order prism {a}, respectively. An ODF calculation has been performed, firstly in order to calculate the orientation of the base pinacoid {c} which could not be directly measured and secondly to separate the positive and negative rhombs {r} and {z} whose pole figures are intrinsically overlapped. A comparison of experimental and calculated pole figures of these principal forms is given in Fig. 2, showing excellent agreement between experimental and calculated pole figures. A detailed interpretation and geological discussion of the texture is given by Ghildiyal et al. (1999).

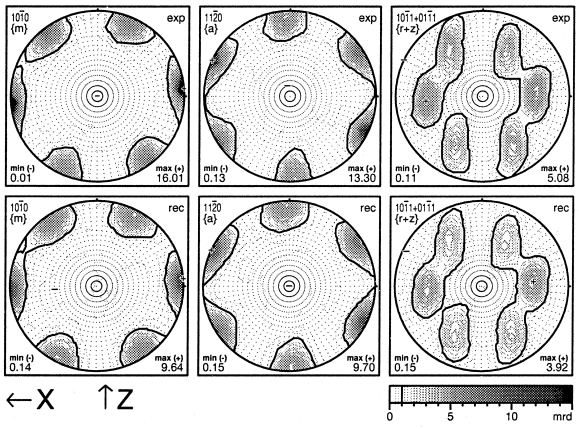

Fig. 2. Observed (top row) and recalculated pole figures (bottom row) of the quartzite showing crystal preferred orientations of the prisms {m} and {a} and of the intrinsically overlapped positive and negative rhombs {r + z}. X indicates the direction parallel to the lineation and Z is perpendicular to the foliation.

The gain in grain statistics when using neutron diffraction is illustrated in Fig. 3, which compares the distribution of *c*-axes obtained by neutron diffraction technique and optical U-stage measurement. The two pole figures exhibit a remarkable similarity. The neutron diffraction pole figure, however, is based on a fast and efficient investigation of all grains of the sample (here about one million grains) rather than on the painstaking optical analysis of about 100 grains.

6. Experimentally and naturally deformed hematite and hematite-quartz rocks

In co-operation within a research project of Professor H. Siemes, Institut für Mineralogie und Lagerstättenlehre, RWTH Aachen, neutron texture investigations have been performed on an experimentally deformed hematite ore

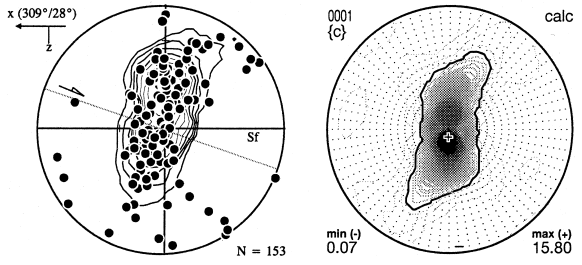

Fig. 3. Comparison of *c*-axis pole figures of the quartzite obtained from U-stage measurements (left) and neutron diffraction (right) as calculated from the ODF.

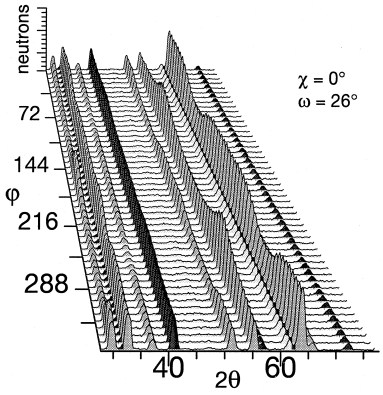

Fig. 4. Intensity variations of hematite-quartz reflections during pole figure scanning (rotation of φ at constant $\chi = 0$) in one fixed detector position; compare Fig. 5 for indexing of quartz (dark) and hematite (light) reflections.

from South Africa (Siemes and Klingenberg, 1998). The natural preferred orientation of this hematite which consists of fine (grain sizes 5–25 μm) and coarse-grained layers (grain sizes 80–175 μm) is characterized by a circular *c*-axis maximum (2.0 mrd) and weak great circle girdles of the prism planes (1.2 mrd). The pole figure measurements were performed on several cylindrical specimens of 10 mm diameter and 15 mm length. After experimental deformation at temperatures between 700°C and 1100°C at $P_c = 300$ MPa and a strain rate of 10^{-4} s^{-1} the specimens were reinvestigated, but then encapsulated in Fe-jackets and Rhenium as prepared for the deformation experiments. The pole figures obtained at and above 700°C indicated different deformation mechanisms (Siemes et al., 1999).

In addition to these measurements, the possibility of analysing a weak texture of a minor component (quartz) in the presence of a major component (hematite) has been tested on a naturally deformed hematite-quartzite ore (cylinder of about 30 mm diameter and height) kindly provided by Professor Quade, TU Clausthal-Zellerfeld. Pole figure scanning of hematite and quartzite reflections

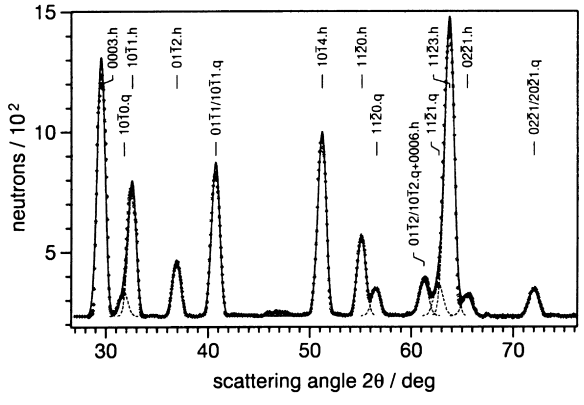

Fig. 5. Neutron diffraction pattern of hematite (h)-quartz (q) measured in one fixed position of the linear detector. The pattern represents the sum diagram over all sample orientations; experimental data points (dots) and profile fit (solid curve).

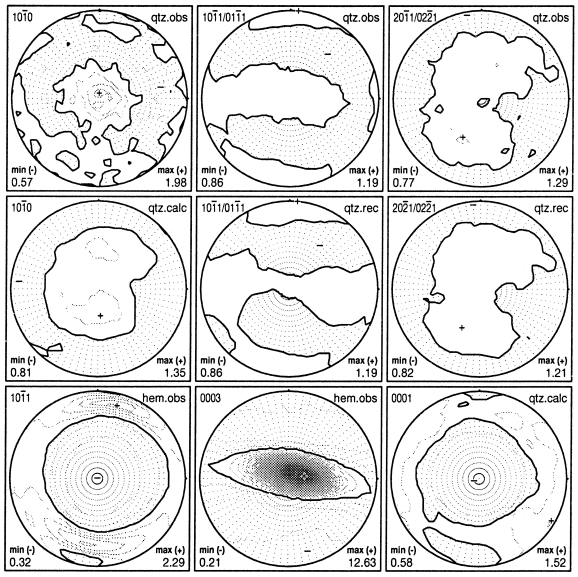

Fig. 6. Top row: Experimental pole figures (10-10), (10-11/01-11) and (20-21/02-21) of the minor quartz component in a hematite-quartz rock. Pole figure (10-10) was not considered in the ODF calculation because of a contamination by the strongly superimposed (10-11/01-11) of the major hematite component (compare Fig. 5). Middle row: Calculated (10-10) and recalculated (10-11/01-11) and (20-21/02-21) of quartz according to the ODF calculation for comparison. Bottom row: Experimental (10-11/01-11) and (0003) pole figures of the major hematite component and, for comparison to the latter, of the calculated (0001) of quartz (right). The different strengths of *c*-axis orientations of both components are illustrated by maximum pole densities of 12.63 mrd and 1.52 mrd of (0003) hem and (0001) qtz, respectively (mrd = multiples of random distribution).

was done simultaneously (Fig. 4). The sum diagram over all sample orientations is shown in Fig. 5. Ensuing ODF calculations for the quartzite component were based on the three experimental pole figures (10-11), (11-20) and (20-21). The comparison of experimental and calculated pole figures in Fig. 6 reveals a fairly well-determined texture.

7. Naturally deformed orthopyroxen-sillimanite-granulite

Complementary U-stage and neutron diffraction measurements have been performed by M. Gastreich (diploma thesis, University of Bonn, in progress) on a granulite rock originating from the Kolivitsa-Umba Satur zone (Kola peninsula). This sample, with grain sizes up to several millimetres, contained the mineral phases orthopyroxen (bronzite), quartz and sillimanite. Diffraction data were collected on a cube-shaped specimen of $2 \times 2 \times 2$ cm^3. Experimental quartz pole figures have been used for ODF calculations (see Fig. 7). A geological interpretation of the rock texture with respect to the three mineral components is given by Gastreich et al. (presented at the Annual Meeting of the Deutsche Gesellschaft für Kristallographie, Aachen, 13–16 March 2000).

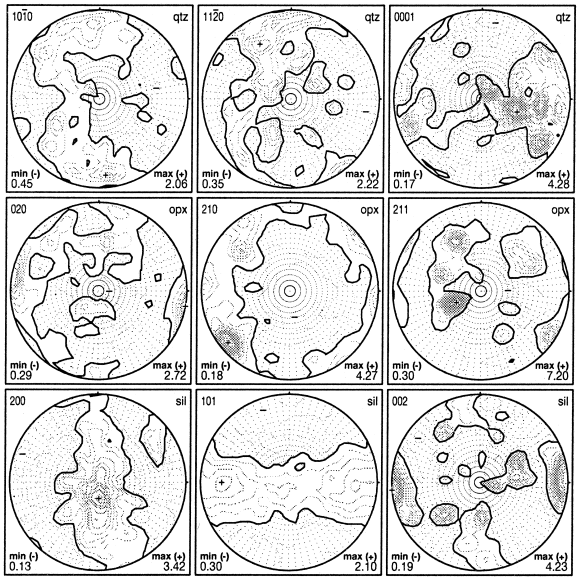

Fig. 7. Experimental pole figures of quartz (qtz, top row), bronzite (opx, middle row) and sillimanite (sil, bottom row) of the orthopyroxen-granulite rock. (0001) of quartz has been calculated from the ODF.

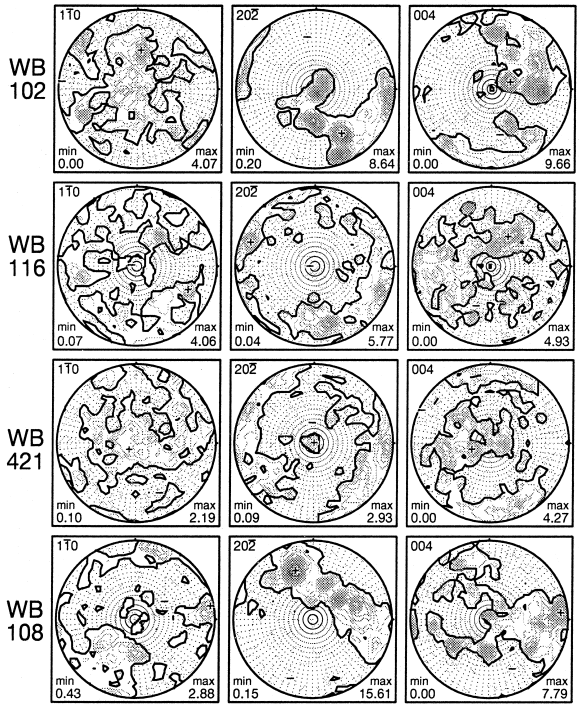

Fig. 8. Comparison of selected experimental pole figures (horizontal) of the four different anorthosite specimens (vertical) classified as ultramylonithic WB102, discrete mylonitic WB116, recrystallized WB421 and partly recrystallized and partly undeformed WB108.

8. Geological anorthosite specimens

Anorthosite specimens originating from different locations of the large massif-type Gruber anorthosite in Central Dronning Maud Land, Antarctica, have been analysed by neutron diffraction pole figures with respect to different deformation strengths (Jansen et al., 2000). The samples were prepared as cubes of 15 mm edge size each. The average composition of the triclinic plagioclase minerals is $An_{54}Ab_{45}Or_{01}$. Diffraction pattern contaminations by other mineral components were negligible. Integrated pole figure intensities were calculated by applying position-constrained profile fitting. For each sample, a total of 15 pole figures of d-spacings between 7 and 3 Å was obtained, the majority being reasonably resolved (Fig. 8). A geological interpretation of the texture is in progress.

9. Conclusions and outlook

The texture diffractometer SV7b equipped with a large linear detector and the Jülich system of specimen-specific pole figure data processing are well suited for texture investigations on geological material. The good performance has been proven on high and low symmetry, on fine- and coarse-grained and on single- and multiphase rocks. The special highlights of neutron diffraction texture analyses are (1) easy sample preparation by just cutting a cube-shaped piece, without any demands on a surface treatment, (2) fast and automatic data collection contrary to the painstaking optical work, (3) simultaneous data collection for the evaluation of a manifold of pole figures, thus gaining additional texture information which is not available by conventional techniques, and (4) the possibility of ODF calculations even for low-symmetry minerals and multiphase rocks, thus establishing a new quality of texture analysis for many geological samples.

For the future, the collection of complete diffraction patterns during pole figure scanning opens up new possibilities in simultaneous crystal structure refinement, texture and quantitative phase analysis. Software developments based on the Rietveld method are in progress (Wenk et al., 1994; Matthies et al., 1997), and programs for time-of-flight data became available recently (Von Dreele, 1997; Lutterotti et al., 1999a,b).

Acknowledgement

Financial support by the BMBF, Bonn, under contract no. 03KI5BO2 is gratefully acknowledged.

References

Bunge, H.J., Wenk, H.-R., Pannetier, J., 1984. Neutron diffraction texture analysis using a 2θ position sensitive detector. Textures and Microstructures 5, 153–170.

Ghildiyal, H., Jansen, E., Kirfel, A., 1999. Volume texture of a deformed quartzite observed with U-stage microscopy and neutron diffractometry. Textures and Microstructures 31, 239–248.

Helming, K., 1996. Texturapproximation durch Modellkomponenten. Cuvillier Verlag, Göttingen.

Jansen, E., Bauer, W., Schäfer, W., 2000. Neutron diffraction pole figures of geological anorthosite textures. Physica B, 276–278, 948–949.

Lutterotti, L., Matthies, S., Wenk, H.-R., 1999a. MAUD (Material Analysis Using Diffraction): a user friedly Java program for Rietveld texture analysis and more. Proceedings of the Twelfth International Conference on Textures of Materials. NRC Research, Ottawa, pp. 1599–1604.

Lutterotti, L., Matthies, S., Wenk, H.-R., 1999b. MAUD: a friendly Java program for material analysis using diffraction. http://www.ing.unitn.it/~luttero

Matthies, S., Lutterotti, L., Wenk, H.-R., 1997. Advances in texture analysis from diffraction spectra. Journal of Applied Crystallograpy 30, 31–42.

Müller, K.D., Reinartz, R., Engels, R., Reinhart, P., Schelten, J., Schäfer, W., Jansen, E., Will, G., 1996. Development of position-sensitive neutron detectors and associated electronics. Journal of Neutron Research 4, 135–140.

Schäben, H., 1994. Diskrete mathematische Methoden zur Berechnung und Interpretation von kristallographischen Orientierungsdichte. DGM Informationsgesellschaft—Verlag Oberursel.

Schäfer, W., Merz, P., Jansen, E., Will, G., 1991. Neutron diffraction texture analysis of multiphase and low-symmetry materials using the position-sensitive detector JULIOS and peak deconvolution methods. Textures and Microstructures 14–18, 65–71.

Schäfer, W., Jansen, E., Skowronek, R., Kirfel, A., 1997. The twin-diffractometer SV7 at the FRJ-2 as a workhorse for structure and texture research. Physica B 234–236, 1146–1148.

Siemes, H., Klingenberg, B., 1998. DFG-project no. Si09-27. Deutsche Forschungsgemeinschaft, Bonn.

Siemes, H., Klingenberg, B., Dresen, G., Rybacki, E., Naumann, M., Schäfer, W., Jansen, E., Rosiere, C.A., 1999. Microstructure and texture of experimentally and naturally deformed hematite ores. ICOTOM 12, 9–13 August 1999, Montreal, Canada

Von Dreele, R.B., 1997. Quantitative texture analysis by Rietveld refinement. Journal of Applied Crystallography 30, 517–525.

Wenk, H.-R., Kern, H., Schäfer, W., Will, G., 1984. Comparison of neutron and X-ray diffraction in texture analysis of deformed carbonate rocks. Journal of Structural Geology 6, 687–692.

Wenk, H.-R., Bunge, H.J., Jansen, E., Pannetier, J., 1986. Preferred orientation of plagioclase-neutron diffraction and U-stage data. Tectonophysics 126, 271–284.

Wenk, H.-R., Mathies, S., Lutterotti, L., 1994. Texture analysis from diffraction spectra. Material Science Forum 157–163, 473–480.

Will, G., Schäfer, W., Merz, P., 1989. Texture analysis by neutron diffraction using a linear position sensitive detector. Textures and Microstructures 10, 375–387.

Will, G., Jansen, E., Schäfer, W., 1992. Texture analysis of bulk samples by neutron diffraction using a position sensitive detector. Advances in X-Ray Analysis 35, 285–291.